

## Crystallographic Analysis of Bacterial Signal Peptidase in Ternary Complex with Arylomycin A<sub>2</sub> and a $\beta$ -Sultam Inhibitor<sup>†,‡</sup>

Chuanyun Luo,<sup>§</sup> Patrick Roussel,<sup>‡</sup> Jürg Dreier,<sup>‡</sup> Malcolm G.P. Page,<sup>‡</sup> and Mark Paetzel<sup>\*,§</sup>

<sup>§</sup>Department of Molecular Biology and Biochemistry, Simon Fraser University, South Science Building 8888 University Drive, Burnaby, British Columbia, V5A 1S6 Canada, and <sup>‡</sup>Basilea Pharmaceutica International Ltd., Grenzacherstrasse 487, CH-4058, Basel, Switzerland

Received June 5, 2009; Revised Manuscript Received August 3, 2009

**ABSTRACT:** Bacterial type I signal peptidase (SPase I), an essential membrane-bound endopeptidase with a unique Ser/Lys dyad mechanism, is being investigated as a potential novel antibiotic target. We present here binding and inhibition assays along with crystallographic data that shows that the lipohexapeptide-based natural product arylomycin A<sub>2</sub> and the morpholino- $\beta$ -sultam derivative (BAL0019193) inhibit SPase I by binding to non-overlapping subsites near the catalytic center. The 2.0 Å resolution crystal structure of the soluble catalytic domain of *Escherichia coli* SPase I (SPase I  $\Delta$ 2–75) in ternary complex with arylomycin A<sub>2</sub> and BAL0019193 reveals the position of BAL0019193 adjacent to arylomycin A<sub>2</sub> within the SPase I binding site. BAL0019193 binds in a noncovalent manner in close proximity to SPase I residues Ser88, Ser90, Lys145, Asn277, Ala279, and Glu307, as well as atom O45 of arylomycin A<sub>2</sub>. The binding mode of arylomycin A<sub>2</sub> in this 2.0 Å resolution ternary complex is compared to that seen in the previous 2.5 Å resolution arylomycin A<sub>2</sub>-SPase cocystal structure. This work contributes to our understanding of SPase I inhibitor/substrate recognition and should prove helpful in the further development of novel antibiotics based on the inhibition of SPase I.

Bacterial type I signal peptidase (SPase I,<sup>1</sup> EC 3.4.21.89) belongs to a family of membrane-bound serine endopeptidases constituting a novel protease clan (SF) and protease family S26 (I), that use a serine/lysine catalytic dyad mechanism instead of a classical serine/histidine/aspartic acid triad catalytic mechanism (2, 3). SPase I is an essential enzyme for bacterial viability. A lack of bacterial SPase I activity leads to an accumulation of exported pre-proteins in the plasma membrane of the cell that eventually results in lysis of the membrane and cell death (4). Therefore, SPase I is being investigated as a target for structure-based rational design of novel antibiotics.

SPase I is not inhibited by the standard serine protease inhibitors; nevertheless, to date, five types of SPase I inhibitors have been discovered. (1) Signal peptides, the N-terminal products of SPase I catalyzed pre-protein cleavage, have been shown to inhibit SPase I in a competitive manner (5). (2) Preproteins that carry signal peptides with a proline at the +1 position (P1')

relative to the cleavage site have been shown to effectively inhibit SPase I (6). (3) A group of  $\beta$ -lactam type (penem) inhibitors (7–9) have been discovered to irreversibly inhibit SPase I by reacting covalently with the nucleophilic serine O<sub>y</sub>. Penems with 5S stereochemistry have the highest potency. The compound allyl (5S,6S)-6-[(R)-acetoxyethyl]-penem-3-carboxylate has an inhibitory concentration (IC<sub>50</sub>) value of less than 1  $\mu$ M against *Escherichia coli* SPase I. The crystal structure of *E. coli* SPase I  $\Delta$ 2–75, a soluble catalytically active fragment of SPase I, has been solved in complex with the 5S-penem (2). (4) Rationally designed lipopeptide based aldehydes have recently been shown to be effective SPase I inhibitors (10). (5) Interestingly, a family of lipohexapeptides isolated from *Streptomyces* sp was shown to be SPase I inhibitors (11–13). These lipohexapeptides have been named arylomycins. The inhibitor arylomycin A<sub>2</sub> has been cocrystallized with *E. coli* SPase I  $\Delta$ 2–75 (14). Arylomycin A<sub>2</sub> consists of two structural features: a hexapeptide (D-MeSer-D-Ala-Gly-L-MeHpg-L-Ala-L-Tyr) and a 12-carbon branched fatty acid (Figure 1A). The first two residues of the peptide have D-stereochemistry. Two of the residues are methylated at the main-chain amide nitrogen (MeSer and MeHpg). The amino acid residue MeHpg is N-methyl-4-hydroxyphenylglycine. Three residues (L-MeHpg-L-Ala-L-Tyr) of the hexapeptide form a macrocyclic ring via a (3,3)-biaryl bridge of the ortho-carbon atom of the MeHpg phenol ring and the ortho-carbon atom of the Tyr phenol ring. The branched 12-carbon fatty acyl chain is attached via an amide bond to the amino terminal D-MeSer of the peptide (Figure 1A). The cocystal structure of arylomycin A<sub>2</sub> bound to *E. coli* SPase I has served as a template for investigations using molecular dynamic simulation techniques (15) and modeling studies (16). Excitingly, the first total synthesis of arylomycin

<sup>†</sup>This work was supported in part by the Canadian Institute of Health Research (to M.P.), the National Science and Engineering Research Council of Canada (to M.P.), the Michael Smith Foundation for Health Research (to M.P.), and the Canadian Foundation of Innovation (to M.P.).

<sup>‡</sup>Atomic coordinates and structure factors have been deposited in the RCSB PDB database with the accession number 3IIQ.

<sup>\*</sup>To whom correspondence should be addressed: Dr. Mark Paetzel, Department of Molecular Biology and Biochemistry, Simon Fraser University, South Science Building 8888 University Drive, Burnaby, British Columbia, V5A 1S6 Canada. Office phone: (778) 782-4230. Lab phone: (778) 782-4318. Fax: (778) 782-5583. E-mail: mpaetzel@sfu.ca.

Abbreviations: ACN, acetonitrile; DCM, dichloromethane; DIPEA, diisopropylethylamine; DMAP, dimethylaminopyridine; DMSO, dimethylsulfoxide; SPase I, type I signal peptidase;  $\Delta$ 2–75, the construct of *E. coli* signal peptidase lacking the residues 2 through 75, which corresponds to the transmembrane segments and the cytoplasmic region.

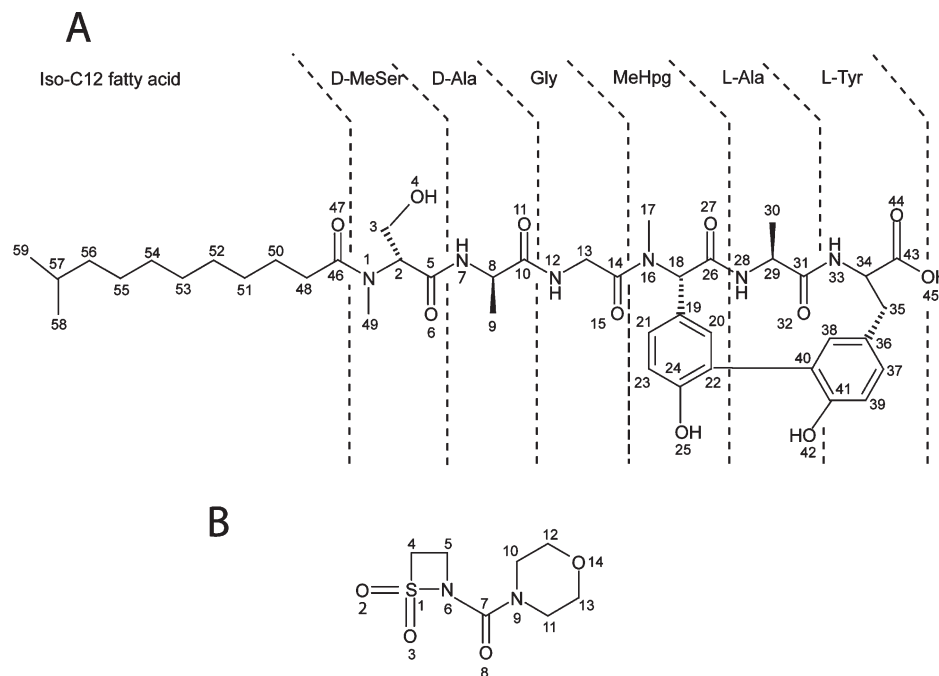


FIGURE 1: Inhibitors in ternary complex with *E. coli* type I signal peptidase. (A) Arylomycin A<sub>2</sub>. (B) The morpholino- $\beta$ -sultam derivative (BAL001913).

A<sub>2</sub> has been reported, which will provide an avenue for the design of arylomycin A<sub>2</sub> analogues (17).

While pursuing analogues of the irreversible,  $\beta$ -lactam-based inhibitors, it was discovered that  $\beta$ -sultams are weak inhibitors of SPase I (Roussel, Dreier, Page, unpublished data). The morpholino derivative, BAL001913 (Figure 1B), was found to inhibit substrate hydrolysis but not to interfere with arylomycin A<sub>2</sub> binding. In order to understand the structural reasons for the independent inhibition of SPase I by these two compounds, we have solved the crystal structure, at 2.0 Å resolution, of arylomycin A<sub>2</sub> and BAL001913 bound to *E. coli* SPase I. The structure reveals that these two inhibitors form a ternary complex in which each forms multiple interactions with the protein but have little interaction with each other.

## MATERIALS AND METHODS

**SPase I  $\Delta$ 2–75, Arylomycin A<sub>2</sub> and BAL001913.** SPase I  $\Delta$ 2–75 was expressed and purified as described previously (18). The concentration of SPase I  $\Delta$ 2–75 was adjusted to 15 mg/mL (0.54 mM), in 20 mM Tris-HCl pH 7.5 and 0.5% Triton-100.

Arylomycin A<sub>2</sub> was isolated from *Streptomyces sp.* from the Basilea strain collection. Stock solutions of arylomycin A<sub>2</sub> were prepared at a concentration of 20 mM in 100% DMSO and stored at  $-80^\circ\text{C}$ .

BAL001913 was synthesized as follows (19): DMAP (0.036 g, 0.3 mmol, 0.2 equiv) and morpholine-4-carbonyl chloride (0.261 mL, 2.24 mmol, 1.5 equiv) were added to a solution of 1,2-thiazetidine-1,1-dioxide (0.160 g, 1.49 mmol) in DCM (15 mL) at  $0^\circ\text{C}$  under a nitrogen atmosphere. After the addition of DIPEA (0.320 mL, 1.87 mmol, 2 equiv), the reaction was allowed to warm up to room temperature for 3 h. After the addition of DCM (8 mL), the mixture was washed with brine and extracted thrice. The organic layers were dried over sodium sulfate and concentrated under reduced pressure. The crude product was purified by flash chromatography (ethyl acetate/cyclohexane: 2/1) to afford BAL001913 (0.220 g, 1 mmol) in a 66.9% yield. The

solid was stored under N<sub>2</sub> at  $-18^\circ\text{C}$ . <sup>1</sup>H NMR (CDCl<sub>3</sub>)  $\delta$  ppm: 4.24 (t,  $J = 7.7$  Hz, 2H, SO<sub>2</sub>–CH<sub>2</sub>), 3.80 (t,  $J = 6.7$  Hz, 2H, thiazetidine N–CH<sub>2</sub>), 3.76–3.73 (m, 4H, 2 O–CH<sub>2</sub>), 3.70–3.66 (m, 4H, 2 morpholine N–CH<sub>2</sub>).  $m/z$  (+ESI): 221.2 ([M + H]<sup>+</sup>, 100%). HPLC: 100% purity by ELSD. An authentic sample of BAL001913 was generously provided by Prof. Michael I. Page (Department of Chemical and Biological Sciences, University of Huddersfield, Queensgate, Huddersfield, HD1 3DH, U.K.). BAL001913 was not stable in DMSO, as a result of a probable DMSO-mediated hydrolysis. However, BAL001913 was shown to be stable in ACN, water and the TRIS buffer within the time frame of the assay. Stock solutions of BAL001913 were prepared at a concentration of 75 mM in 100% acetonitrile.

**In Vitro SPase I Activity Assay.** The activity of purified SPase I  $\Delta$ 2–75 was measured by following the cleavage of a fluorogenic peptide substrate (20). The IC<sub>50</sub> was determined by curve fitting with GraFit software (Leatherbarrow, R. J., 2001 GraFit Version 5, Erithacus Software Ltd., Horley, U.K.) using eq 1,

$$y = \frac{\text{range}}{1 + \left(\frac{x}{\text{IC}_{50}}\right)^s} \quad (1)$$

where  $y$  is the enzyme activity at an inhibitor concentration  $x$ , range is the fitted uninhibited value and  $s$  is a slope factor.

**Inhibitor Binding Assays.** To investigate the competition between the  $\beta$ -sultam and arylomycin A<sub>2</sub>, 3.7  $\mu\text{M}$  SPase I  $\Delta$ 2–75 was incubated with different concentrations of BAL001913 in 20 mM Tris-HCl pH 7.4, 5 mM MgCl<sub>2</sub>, 0.5% DMSO, 0.8% acetonitrile. The volumes of control reactions without inhibitor were adjusted with buffer. After 30 min at  $25^\circ\text{C}$ , 10  $\mu\text{M}$  arylomycin A<sub>2</sub> was added and the reaction was incubated for another 5 min. Fluorescence emission scans were recorded from 300 to 550 nm using a Perkin-Elmer LS 50B spectrometer with excitation at 280 nm.

**Cocrystallization.** Before setting up crystallization screens, SPase I  $\Delta$ 2–75 was mixed with BAL 001913 (5 molar excess of

BAL 0019193) and the solution was incubated on ice for one hour. Arylomycin A<sub>2</sub> solution was then added to the BAL0019193/SPase I Δ2–75 mixture at a 1:1 molar ratio. The ternary mixture solution of SPase I Δ2–75/arylomycin A<sub>2</sub>/BAL0019193 was kept on ice for one additional hour.

The initial screening for cocrystallization conditions was performed by the sitting-drop vapor-diffusion method at 18 °C using commercial Hampton Research crystallization screens. The final optimized reservoir condition that produced diffraction quality crystals was 0.2 M ammonium formate, 25% PEG 2000, 0.1 M sodium cacodylate pH 6.5, and 5% tertiary-amyl alcohol. The drop was set up with 2 μL of the protein and inhibitor mixture (described above), and 2 μL of the reservoir solution. The drop was equilibrated over 1 mL of reservoir solution.

**Crystallographic Data Collection.** Before data collection, the crystal was transferred by pipet from the growth drop to a cryoprotectant composed of 0.2 M ammonium formate, 25% PEG 2000, 0.1 M sodium cacodylate pH 6.5, 5% tertiary-amyl alcohol, and 20% v/v glycerol and incubated for two days. The data set was collected on beamline 8.2.2 at the Advanced Light Source of Lawrence Berkeley National Laboratory, using a Quantum-315 ADSC detector. The X-ray wavelength was 1.1217 Å. The crystal was rotated 100°, with a 1.0° oscillation per frame. The exposure time used for each image was 10 s. The crystal to detector distance was 300 mm. The data revealed significant diffraction to a resolution of 2.0 Å. Data were indexed, integrated, and scaled using the program HKL2000 (21). The crystals belong to the tetragonal space group *P*4<sub>3</sub>2<sub>1</sub>2. The unit cell dimensions were determined to be *a* = 70.0 Å, *b* = 70.0 Å, and *c* = 259.9 Å. The Matthews coefficient (*V*<sub>m</sub>) is 2.88 Å<sup>3</sup>/Da for two molecules in the asymmetric unit. The fraction of the crystal volume occupied by solvent was 56.5% calculated by the program *Matthews* in the CCP4i suite of program (22, 23). For crystal and data collection statistics see Table 1.

**Phasing, Model Building, and Refinement.** A molecular replacement solution was found using CaspR (24). PDB atomic coordinates 1T7D (protein chain A with all ligands removed) were used as the search model (14). The topology and parameter files for the inhibitor coordinates were generated using the program PRODRG (25). Atomic coordinates for arylomycin A<sub>2</sub> and BAL0019193 were manually docked into electron difference densities (*F*<sub>o</sub> – *F*<sub>c</sub>) near the active site. In addition, the main chain trace and the side chain assignments for the dynamic regions corresponding to residue Ser197–Asn200 in molecule B and residues 304–314 in both molecule A and B were built manually. Model building and analysis was performed with the program XFIT in the suite XTALVIEW and the program COOT (26, 27). Cycles of refinement were carried out using rigid body refinement followed by restrained NCS refinement in Refmac 5, and simulated annealing, energy minimization, and *B*-factor refinement in CNS (23, 28). In addition, a cycle of TLS refinement was carried out using the TLS Motion Determination Server and TLS-restrained refinement with Refmac 5 within the CCP4i suite (23, 29). In all cycles of refinement, 5% of the reflections were set aside for cross-validation. Final refinement and analysis statistics of this ternary complex are provided in Table 1.

**Structural Analysis.** The stereochemistry of the structure was analyzed with the program PROCHECK (30). Superposition of structures was performed by the program SuperPose (31). The measurement of the substrate binding site was calculated using

Table 1: Crystallographic Data Collection and Refinement Statistics for the Ternary Complex Structure of SPase I Δ2–75/Arylomycin A<sub>2</sub>/BAL 0019193<sup>a</sup>

Data Collection	
wavelength (Å)	1.1217
space group	<i>P</i> 4 <sub>3</sub> 2 <sub>1</sub> 2 (No. 96)
unit-cell dimensions (Å)	<i>a</i> = 70.0, <i>b</i> = 70.0, <i>c</i> = 259.9
molecules in asu	2
resolution range (Å)	67.4–2.0 (2.14–2.04)
<i>V</i> <sub>m</sub> (Å <sup>3</sup> /Da)	2.88
% solvent	56.5%
total observed reflections	285869
unique reflections	40272
redundancy	7.1 (4.3)
completeness (%)	95.2 (95.1)
<i>R</i> <sub>merge</sub> (%)	6.8(43.0)
mean <i>I</i> /σ( <i>I</i> )	10.4 (5.1)
Refinement	
protein residues	469
atoms	3943
waters	252
<i>R</i> <sub>work</sub>	20.7
<i>R</i> <sub>free</sub>	25.0
rms deviations	
bonds (Å)	0.030
angles (deg)	2.348
estimated overall coordinate error (Å)	0.181
average <i>B</i> (Å <sup>2</sup> ) for protein atoms	chain A, 36.3; chain B, 39.2
average <i>B</i> (Å <sup>2</sup> ) for water atoms	49.5
average <i>B</i> (Å <sup>2</sup> ) for inhibitors	in chain A, 54.0; in chain B, 64.2

<sup>a</sup>*R*<sub>merge</sub> =  $\sum |I_{o,i}| - |I_{ave,i}| / \sum |I_{ave,i}|$ , where *I*<sub>ave,i</sub> is the average structure factor amplitude of reflection *I* and *I*<sub>o,i</sub> represents the individual measurements of reflection *I* and its symmetry equivalent reflection. *R*<sub>work</sub> =  $\sum |F_{obs} - F_{calc}| / \sum F_{obs}$ . *R*<sub>free</sub> =  $\sum_{hkl \in T} (|F_{obs}| - |F_{calc}|)^2 / \sum_{hkl \in T} |F_{obs}|^2$ , where  $\sum_{hkl \in T}$  are reflections belonging to a test set of 5% of the data, and *F*<sub>obs</sub> and *F*<sub>calc</sub> are the observed and calculated structure factors, respectively. The data collection statistics in brackets are the values for the highest resolution shell (2.14–2.04 Å).

the program CASTp, and the Accessible Surface Areas (ASA) was calculated by the program AREAIMOL within the CCP4i suite (32, 33). In both CASTp and AREAIMOL, a solvent probe radius of 1.4 Å was used.

**Figure Preparation.** Figures were prepared using program ISIS Draw version 2.5 (MDL Information System, Inc.), XFIT (26), Raster 3D (34) and PyMol (35).

## RESULT AND DISCUSSION

**Binding of Inhibitors to SPase I in Solution.** The morpholino-β-sultam (BAL0019193) inhibited SPase I Δ2–75 in a dose dependent manner with an IC<sub>50</sub> of 610 ± 18 μM (Figure 2A). Arylomycin A<sub>2</sub> inhibits SPase I Δ2–75 with an IC<sub>50</sub> of 1 ± 0.2 μM (14).

Arylomycin A<sub>2</sub> fluoresces at 418 nm when excited at 280 nm. This fluorescence signal was shown to increase significantly upon binding to SPase I Δ2–75, which allows for direct binding measurements (14).

Competition between arylomycin A<sub>2</sub> and the β-sultam inhibitor for binding to SPase I Δ2–75 was investigated by measuring fluorescence at 418 nm. Figure 2B shows fluorescence emission spectra of the β-sultam and arylomycin A<sub>2</sub> inhibitors alone and bound to SPase I Δ2–75. The assay was performed with saturating arylomycin A<sub>2</sub> (10 μM) and concentrations up to 1 mM of the β-sultam molecule, which inhibited the enzymatic



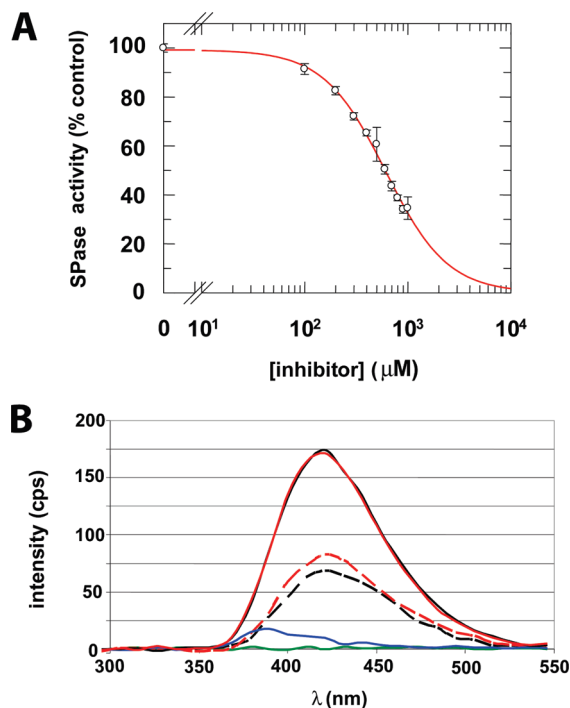


FIGURE 2: (A) Dose dependence of SPase I  $\Delta 2$ –75 inhibition by the morpholino- $\beta$ -sultam inhibitor. The red curve shows a fit described by eq 1. (B) Fluorescence emission spectra of SPase I  $\Delta 2$ –75 and inhibitors, alone and in various combinations (excitation at 280 nm). The blue line corresponds to SPase I  $\Delta 2$ –75 alone. The green line corresponds to the morpholino- $\beta$ -sultam alone. The dashed black line corresponds to arylomycin  $A_2$  alone. The dashed red line corresponds to arylomycin  $A_2$  and morpholino- $\beta$ -sultam together. The black line corresponds to SPase I  $\Delta 2$ –75 with arylomycin  $A_2$ . The red line corresponds to SPase I  $\Delta 2$ –75 with morpholino- $\beta$ -sultam and arylomycin  $A_2$ . The fluorescence was measured in arbitrary units as counts per second.

reaction by  $65.4 \pm 4.6\%$ . No decrease of the arylomycin  $A_2$  fluorescence signal at 418 nm was detected at the highest concentration of BAL0019193 tested. The fluorescence signal of enzyme-bound arylomycin  $A_2$  remained stable for at least 2 h even in the presence of the  $\beta$ -sultam inhibitor. The absence of detectable competition between the two compounds suggested two independently occupied binding sites, both of which interfere with the reaction of SPase I with its substrate. These inhibitors do not exhibit any observable synergy in these mixed competition experiments.

**Cocrystallization, Structure Solution, and Refinement.** Cocrystallization conditions for the ternary complex of SPase I  $\Delta 2$ –75/arylomycin  $A_2$ /BAL0019193 were obtained in the novel condition; 0.2 M ammonium formate, 25% PEG 2000, 0.1 M sodium cacodylate pH 6.5, and 5% tertiary-amyl alcohol. The crystals are box (or parallelepiped) shaped, approximately  $0.3 \times 0.3 \times 0.4$  mm in size, and belong to the space group  $P4_32_12$  with unit cell dimensions of  $a = 70.0$  Å,  $b = 70.0$  Å, and  $c = 259.9$  Å. The crystals gave ordered diffraction to beyond 2.0 Å resolution, and the crystal structure was solved by molecular replacement. The final refinement yielded a model that fits to the experimental electron density with  $R_{\text{cryst}} = 20.7\%$  and  $R_{\text{free}} = 25.0\%$  at 2.0 Å resolution. In the final model, the dynamic surface loops (residues 106–125, 171–177, 196–205) are incomplete or missing due to a lack of electron density for these residues. Two arylomycin  $A_2$  molecules, two  $\beta$ -sultam molecules, two Triton X-100 detergent molecule fragments, four glycerol molecules,

and two acetonitrile molecule were included in the model during the end stages of refinement. Superposition of the two SPase I molecules in the asymmetric unit yields a root mean square deviation (rmsd) value of 0.96 Å ( $\alpha$  carbon, C $\alpha$ ), 1.02 Å (backbone). The structure refinement statistics are summarized in Table 1.

**Arylomycin  $A_2$ /SPase I Interactions in the Ternary Complex.** The ternary complex crystal structure presented here at 2.0 Å resolution reveals an enhanced view of arylomycin  $A_2$  in the binding cleft of SPase I when compared to a previously determined 2.5 Å cocrystal structure of arylomycin  $A_2$  alone in complex with *E. coli* SPase I (14). After completing one cycle of simulated annealing refinement with CNS, the electron density for the complete arylomycin  $A_2$  including the 12-carbon fatty acid of arylomycin  $A_2$  was clearly observed in the SPase binding cleft (in molecule A, Figure 3). The previous structure of SPase I alone with arylomycin  $A_2$  did not reveal electron density for the fatty acid (14). The dihedral angle about the C48–C50 bond within the inhibitor is approaching an eclipsed conformation resulting in the fatty acid having a curved structure (Figure 3). The methylene groups of the fatty acid make van der Waals interaction with part of a large hydrophobic surface (inhibitor atoms C50–52, C53, C58, and C59 contact SPase I residues Pro 83, Gln 85, Phe 100 and Trp 300 respectively) (Figures 3–6). This region of SPase I corresponds to the predicted membrane association surface (2). Interestingly, an amino-terminal fatty acid has been found to improve the effectiveness of both SPase I substrates and inhibitors. For example, a recent report on peptide aldehyde inhibitors of SPase I showed that the amino-terminal decanoyl fatty acid chain of the lipopeptides was critical for its activity (10). It is possible that the fatty acid at the amino-terminus of SPase I peptide substrates and inhibitors helps to orientate the peptide relative to the SPase I binding cleft, mimicking the hydrophobic region of the signal peptide at the amino-terminus of pre-protein substrates *in vivo*. It is also possible that the fatty acid helps the lipopeptide to partition into the hydrophobic milieu of the detergent micelle upon which SPase I is most likely traveling in solution *in vitro*. Even the so-called “soluble catalytic domain” of SPase I, which lacks the two transmembrane anchor regions, requires detergent for optimal activity and crystallization(36, 37).

The noncovalently bound arylomycin  $A_2$  buries an average of  $487.8$  Å<sup>2</sup> of solvent accessible surface area on SPase I  $\Delta 2$ –75. The inhibitor is positioned in the binding pocket in a similar orientation to what was seen previously in the 2.5 Å resolution structure (14), with its C-terminus (the 3-residue biaryl-bridged ring system, MeHpg-L-Ala-L-Tyr) pointing toward the active site, and makes a parallel  $\beta$ -strand interaction with a  $\beta$ -strand (residues 142–145) that lines the SPase I binding cleft. The main chain of the N-terminus of the inhibitor (D-MeSer-D-Ala-Gly) makes interactions with  $\beta$ -strand 83–90 that lines the other side of the binding cleft (Figures 4A,B and 5). The C-terminal carboxylated oxygen atom O45 interacts with three catalytic residues including the nucleophile Ser90 O $\gamma$ , the general base Lys145 N $\zeta$ , and the oxyanion hole Ser88 O $\gamma$ . Its carbonyl oxygen atom O44 is hydrogen-bonded to Ile144 N and the general base Lys145 N $\zeta$ . The N-terminal end of the 3-residue biaryl-bridged ring system (MeHpg-L-Ala-L-Tyr) makes hydrogen bonding interactions through N33, N28, O27, O15, O11, N7, and O4 to protein residues Asp142, Ser88, Gln85, Phe84, Pro83, and Glu82. The hydrogen bond from O27 of the inhibitor to the residue Asp142 N is through a

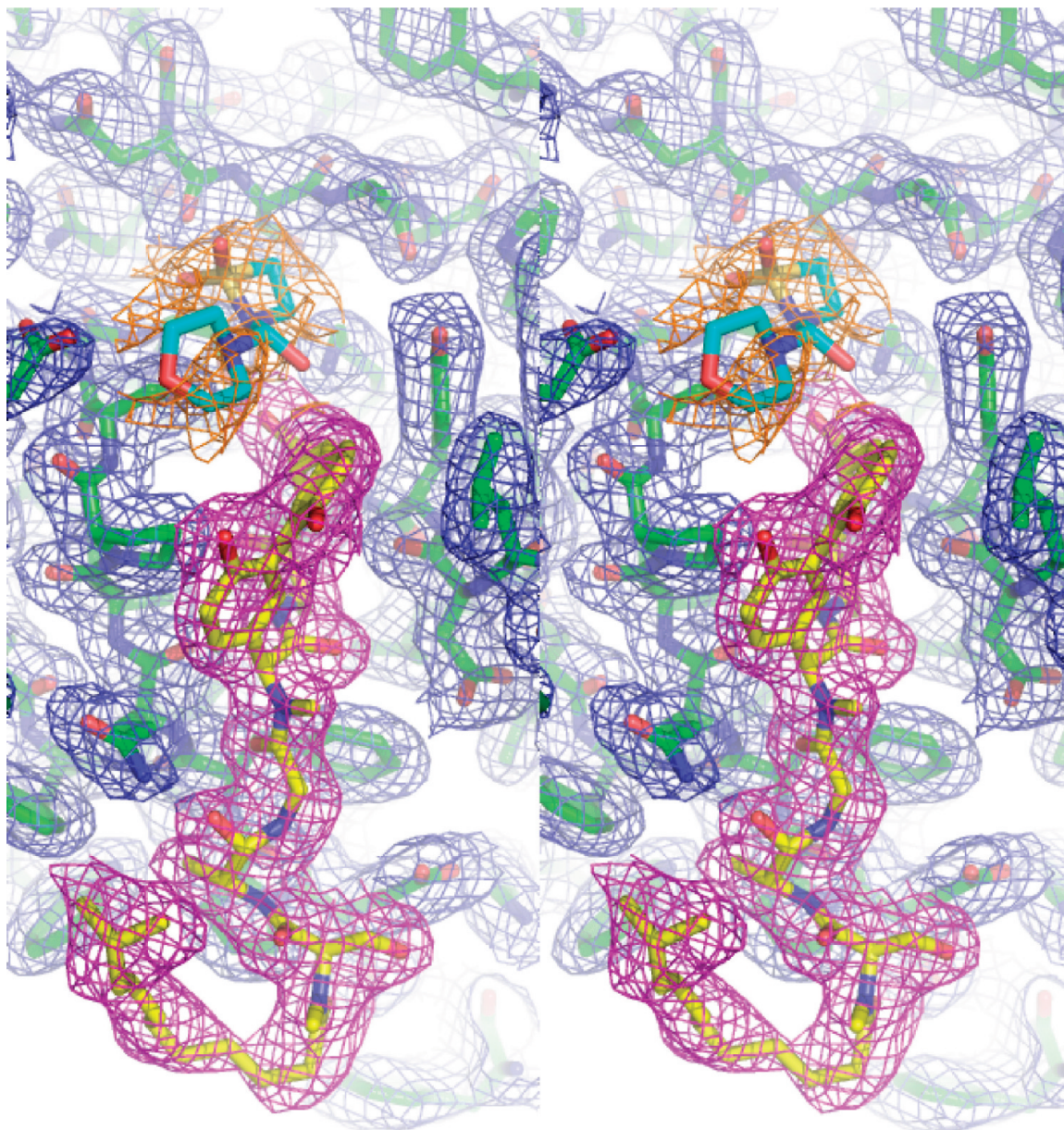


FIGURE 3: A stereoview of the electron density for the inhibitors arylomycin  $A_2$  and BAL0019193 bound at the active site of *E. coli* SPase I. A cross-validated  $2F_o - F_c$  electron density map contoured at  $0.5\sigma$  surrounds the inhibitor arylomycin  $A_2$  (magenta), BAL0019193 (orange) and protein (blue). The carbon atoms of arylomycin  $A_2$  are in yellow, the carbon atoms of BAL0019193 are in cyan, and the protein has carbon atom in green. The oxygen atoms are in red, and nitrogen atoms are in blue. The inhibitors shown here are from molecule A.

water molecule (water 362 in molecule A and water 365 in molecule B). Water molecule 5 links inhibitor atom O32 to the  $O\gamma$  and NH of Ser88.

There are several van der Waals interactions observed to assist the molecular recognition of arylomycin  $A_2$  by SPase I. Most notably, the C30 methyl group from the Ala side chain of arylomycin  $A_2$  points into the S3 substrate-binding pocket of SPase I.

A superposition of the 2.0 Å ternary arylomycin  $A_2$ /BAL0019193/SPase I complex structure presented here with the previously solved 2.5 Å resolution binary arylomycin  $A_2$ /SPase I complex structure reveals that the position of the arylomycin  $A_2$  in the ternary complex is slightly shifted ( $\sim 0.2$  Å) away from the catalytic residues in the ternary complex. The N-termini of the lipohexapeptide adopt similar geometries in the two structures, but one is shifted slightly in path with respect to the other, beginning with atom C13 down to atom C48.

The subtle binding mode differences may be a result of the steric constraints imposed by the BAL0019193 binding adjacent to the biaryl-ring moiety of the arylomycin  $A_2$ .

**The Binding Mode for the  $\beta$ -Sultam Inhibitor.** Remarkably, given the underlying mechanistic hypothesis (19) and previous experience with  $\beta$ -lactamases and D,D-peptidases (38, 39), which also use Ser/Lys catalytic activation, BAL0019193 was best refined as the unreacted molecule, with the  $\beta$ -sultam ring intact. The  $F_o - F_c$  and omit electron density maps near the binding site are consistent with BAL0019193 being located above the active site and taking a parallel orientation relative to the biaryl ring moiety of arylomycin  $A_2$  (Figures 3 and 4). BAL0019193 appears to be noncovalently bound, there is no electron density continuous with the nucleophilic Ser90 $O\gamma$ . BAL0019193 has an occupancy of approximately 0.5. The electron density surrounding BAL0019193 is incomplete in regions near the morpholino group. This could be a result of the inhibitor being more dynamic in this



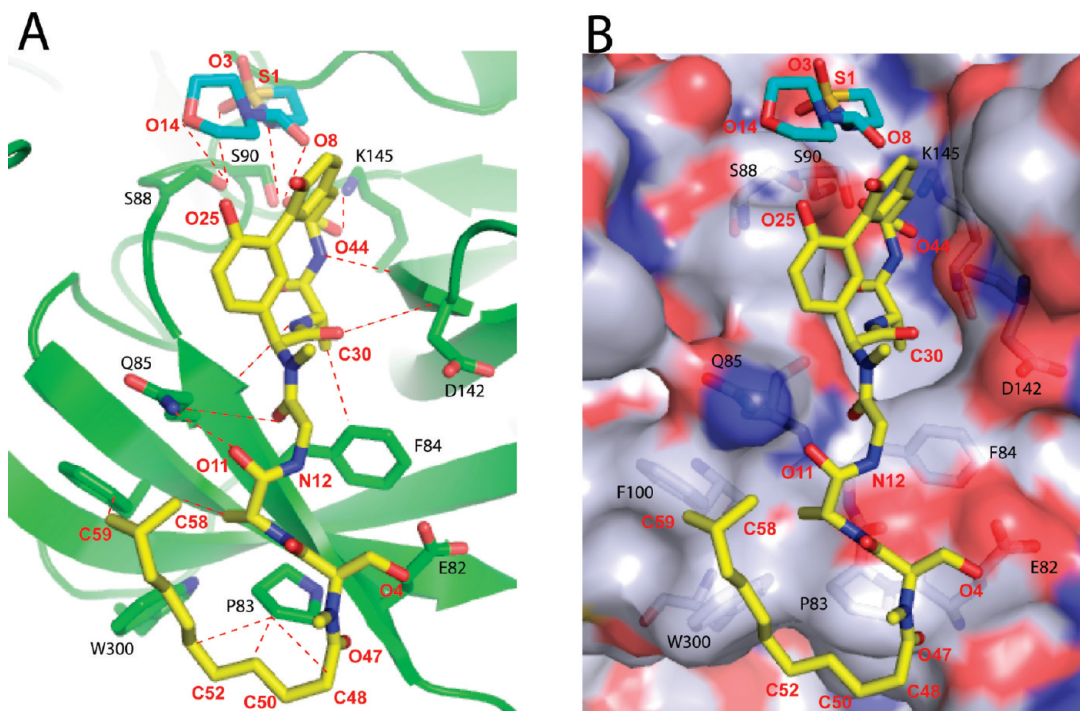


FIGURE 4: The overall binding theme of arylomycin A<sub>2</sub> and BAL0019193. (A) SPase I is in ribbon representation and colored in green. Inhibitor arylomycin A<sub>2</sub> is represented as stick and colored by element with carbon atoms in yellow, nitrogen atoms in blue, and oxygen atoms in red. Inhibitor BAL0019193 is represented as stick and colored by element with carbon atoms in cyan, nitrogen atoms in blue, and oxygen atoms in red. (B) A semitransparent molecular surface representation of SPase I with the following color scheme: basic residues are in blue, acidic residues are in red, all others are in gray. Inhibitors are represented and colored the same as that in diagram A. The red labels are for the inhibitor atoms and the black labels are for the SPase I residues in one letter code.

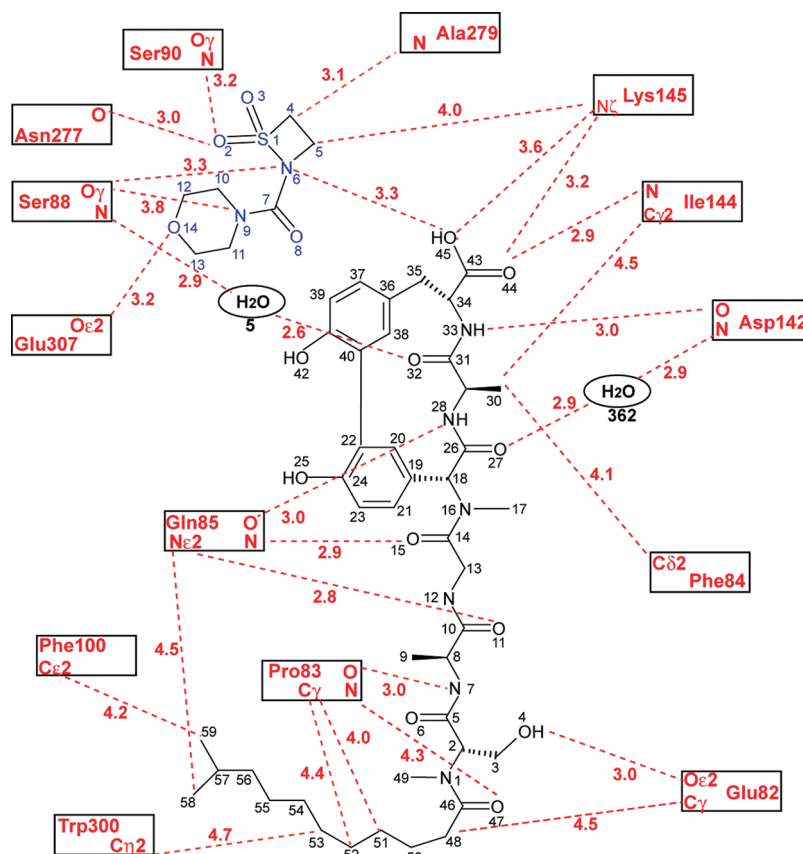


FIGURE 5: A schematic diagram of the interactions observed between arylomycin A<sub>2</sub> and BAL0019193 and SPase I Δ2–75 (molecule A).

region. In addition, although the  $\beta$ -sultam refined best as the nonhydrolyzed form, it is possible that there maybe a mixed

population of hydrolyzed and nonhydrolyzed BAL0019193 occupying the binding site. As modeled, BAL0019193 buries

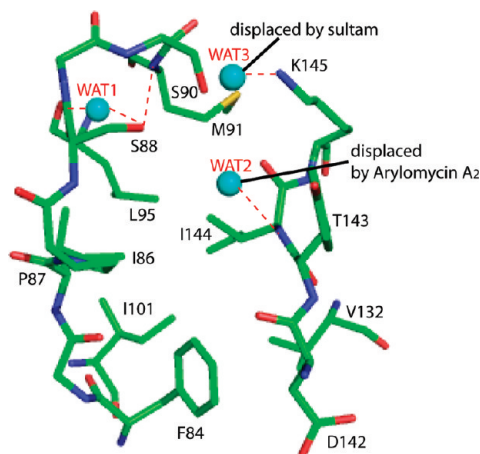


FIGURE 6: The three conserved water molecules in the active site of *E. coli* SPase I. The residues near the active site and binding cleft (subsites S1 and S3) of SPase I are represented in stick and colored by element: carbon, green; nitrogen, blue; oxygen, red. The three conserved waters are shown as cyan colored spheres. The hydrogen bonding interactions between the waters and the residues of SPase I are indicated by red dashed lines. The waters that are displaced by bound inhibitors are indicated. Water 3 (WAT3) is the proposed deacylating water. This figure was prepared using molecule A from the apoenzyme crystal structure of SPase I (PDB code: 1KN9) (40)

approximately 187 Å<sup>2</sup> of solvent accessible surface area on SPase I Δ2–75. BAL0019193 interacts with both SPase I and the inhibitor arylomycin A<sub>2</sub>. Atoms S1, O2, N6, N9, and O8 of BAL0019193 are close to residues Ser88, Ser90, Lys 145, Asn 277, Ala279, and Glu307 of SPase I Δ2–75, and O45 of arylomycin A<sub>2</sub> (Figure 5 and table in the Supporting Information). Interestingly, the atoms S1, O2, N6, N9, and O8 of BAL0019193 reside close to the catalytic residue atoms Ser88 O<sub>γ</sub> and Ser90 N that are involved in the formation of the oxyanion hole. The molecular interactions between SPase I and the inhibitor arylomycin A<sub>2</sub> as well as inhibitor BAL0019193 are shown in Figure 5 and the table in the Supporting Information.

**Active-Site Waters.** The crystal structure of SPase I with an empty binding cleft (the apo-structure) (40) revealed three conserved water molecules near the active site (designated as water 1, water 2, and water 3). Water 1 is coordinated to the Met 91 backbone NH, Ser88 O, and Leu95 O. Water 2 is coordinated to Ile144 NH. Water 3 is coordinated to the N<sub>ζ</sub> of Lys145 and is hypothesized to function as the deacylating water in the SPase I catalysis (40). For convenience, the apoenzyme numbering of the conserved active site waters is kept for the structure presented here (Figure 6). In the β-lactam acyl–enzyme structure, water 1 was present, but waters 2 and 3 were displaced by the β-lactam inhibitor (2). In the arylomycin A<sub>2</sub> cocrystal structure, water 1 and water 3 were present, but water 2 was displaced by arylomycin A<sub>2</sub> (O44) (14). In the ternary arylomycin A<sub>2</sub>/BAL0019193/SPase I complex structure, only water 1 is present. Water 2 is displaced by the atom O44 of arylomycin A<sub>2</sub>, and water 3 is displaced by atom C5 of BAL0019193 (Figure 6). It is possible that the displacement of water 3 by BAL0019193 may explain its inhibitory activity without the need to react with the nucleophile. The cocrystallization with both arylomycin A<sub>2</sub> and BAL0019193 resulted in a considerable increase in crystal order and thus diffraction quality when compared to the previously determined binary complex with arylomycin A<sub>2</sub> alone. This suggests that BAL0019193 stabilizes the arylomycin A<sub>2</sub> interaction with SPase I and results in a more

rigid structure. Weak inhibitors such as BAL0019193 normally make bad starting points as drug leads and are therefore usually only pursued if they indicate a new mode of inhibition that can be exploited by other means. The observation of the ternary complex reported here does indeed offer this possibility by defining novel space and interactions around the catalytic center that could be filled by appropriate design.

**Cocrystallization with Inhibitors and Ligands Provide Clues to Pre-Protein Substrate Binding Subsites.** A superposition of the covalently bound β-lactam (5S-penem) complex structure with the ternary complex structure (inhibitors arylomycin A<sub>2</sub> and β-sultam and detergent) shows that the β-lactam inhibitor clashes with the C-terminal portion of the arylomycin A<sub>2</sub> revealing that the penem and the lipopeptide would not be effective together. The superposition also shows how the penem positions a methyl group into the S1 subsite, whereas the arylomycin A<sub>2</sub> positions a methyl group into the S3 subsite. This is consistent with the SPase I preference for small aliphatic residues at the P1 and P3 positions within the pre-protein substrates. The hexapeptide of arylomycin A<sub>2</sub> makes β-sheet type hydrogen bonding interactions with the SPase I binding cleft, much like the classical type of interactions seen in serine protease substrate complexes (41). The β-sheet interactions also explain the lack of preference at the P2 position within the signal peptide of the pre-protein substrates. The N-terminal end of the peptide leads to a potential S7 subsite which is in proximity to a critical Trp300 residue that resides along the proposed membrane association surface(42). The protein architecture of the SPase I catalytic core is very similar to the self-cleaving *lexA* repressor whose structure was solved with its cleavage site region bound in its binding site(43). This provided an opportunity to model a signal peptide into the binding site of SPase I based on the *lexA* structure (44). The path taken by the arylomycin A<sub>2</sub>/β-lactam superposition shown here is in good agreement with the modeled signal peptide(44). Recently a theoretical model of a pre-protein/SPase I complex was published based on the structures of SPase I inhibitor complexes (16). The model includes subsites on both sides of the active site; both S and the S' subsites. Our observation of electron density for a Triton X-100 fragment within a crevice along the surface of SPase I just beyond the active site (opposite side from the S1 and S3 subsites, in molecule B) may provide a clue to the location of possible S' subsites (Figure 7).

**Concluding Remarks.** The binding and inhibition assays and structural observations presented here show that type I signal peptidase can be inhibited by two separate inhibitors at the same time via binding to non-overlapping subsites near the catalytic center. This information opens up new possibilities for further structure based design of signal peptide inhibitors that may lead to a novel class of antibiotics. Arylomycin A<sub>2</sub> may function as a competitive inhibitor in that it occupies, in a noncovalent manner, the binding cleft of SPase I. In addition, arylomycin A<sub>2</sub> may be providing a form of transition state intermediate analogue inhibition in that the anionic C-terminal carboxylate oxygens (O45 and O44) hydrogen bond to the catalytically important residues within the SPase I active site (Lys145, Ser90 and Ser88). Sultam-based inhibitors were designed as acylating agents to mimic the acyl–enzyme complex of the serine β-lactamase family. Yet the β-sultam inhibitor used in this work appears to function in a novel way, not by covalently reacting with the nucleophile but rather by binding to a site adjacent to the active site and possibly displacing the deacylating water. Future work will investigate the possibility of covalently tethering

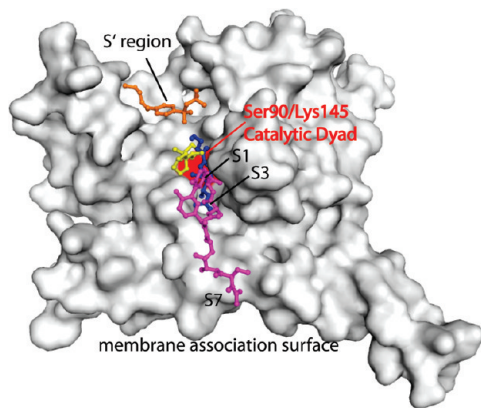


FIGURE 7: A superposition of the  $\beta$ -lactam (5S-penem) inhibitor bound signal peptidase structure (pdb: 1B12, molecule A) (2) on the  $\beta$ -sultam/arylomycin A<sub>2</sub>/SPase I ternary complex structure (molecule B). SPase I is shown as white molecular surface with the catalytic dyad Ser90/Lys145 highlighted in red. The 5S-penem inhibitor is shown in magenta ball-and-stick, the arylomycin A<sub>2</sub> inhibitor is shown as yellow ball-and-stick. A bound fragment of Triton X-100 is shown in orange ball-and-stick. The approximate positions of the proposed substrate binding subsites are labeled.

various chemical groups to the biaryl ring system of arylomycin A<sub>2</sub> such that they would occupy the binding surface on SPase I that we observe BAL0019193 occupying. This may combine various forms of inhibition into a single inhibitor, thus improving its effectiveness.

## SUPPORTING INFORMATION AVAILABLE

A table as described in the text. This material is available free of charge via the Internet at <http://pubs.acs.org>.

## REFERENCES

- Barrett, A. J., and Rawlings, N. D. (1995) Families and clans of serine peptidases. *Arch. Biochem. Biophys.* 318, 247–250.
- Paetzel, M., Dalbey, R. E., and Strynadka, N. C. (1998) Crystal structure of a bacterial signal peptidase in complex with a beta-lactam inhibitor. *Nature* 396, 186–190.
- Paetzel, M., and Strynadka, N. C. (1999) Common protein architecture and binding sites in proteases utilizing a Ser/Lys dyad mechanism. *Protein Sci.* 8, 2533–2536.
- Dalbey, R. E., and Wickner, W. (1985) Leader peptidase catalyzes the release of exported proteins from the outer surface of the *Escherichia coli* plasma membrane. *J. Biol. Chem.* 260, 15925–15931.
- Wickner, W., Moore, K., Dibb, N., Geissert, D., and Rice, M. (1987) Inhibition of purified *Escherichia coli* leader peptidase by the leader (signal) peptide of bacteriophage M13 procoat. *J. Bacteriol.* 169, 3821–3822.
- Barkocy-Gallagher, G. A., and Bassford, P. J. (1992) Synthesis of precursor maltose-binding protein with proline in the +1 position of the cleavage site interferes with the activity of *Escherichia coli* signal peptidase I in vivo. *J. Biol. Chem.* 267, 1231–1238.
- Kuo, D., Weidner, J., Griffin, P., Shah, S. K., and Knight, W. B. (1994) Determination of the kinetic parameters of *Escherichia coli* leader peptidase activity using a continuous assay: the pH dependence and time-dependent inhibition by beta-lactams are consistent with a novel serine protease mechanism. *Biochemistry* 33, 8347–8354.
- Black, M. T., and Bruton, G. (1998) Inhibitors of bacterial signal peptidases. *Curr. Pharm. Des.* 4, 133–154.
- Allsop, A., Brooks, G., Edwards, P. D., Kaura, A. C., and Southgate, R. (1996) Inhibitors of bacterial signal peptidase: a series of 6-(substituted oxyethyl)penems. *J. Antibiot. (Tokyo)* 49, 921–928.
- Buzder-Lantos, P., Bockstael, K., Anne, J., and Herdewijn, P. (2009) Substrate based peptide aldehyde inhibits bacterial type I signal peptidase, *Bioorg. Med. Chem. Lett.*
- Schimana, J., Gebhardt, K., Holtzel, A., Schmid, D. G., Sussmuth, R., Muller, J., Pukall, R., and Fiedler, H. P. (2002) Arylomycins A and B, new biaryl-bridged lipopeptide antibiotics produced by *Streptomyces* sp. Tu 6075. I. Taxonomy, fermentation, isolation and biological activities. *J. Antibiot. (Tokyo)* 55, 565–570.
- Holtzel, A., Schmid, D. G., Nicholson, G. J., Stevanovic, S., Schimana, J., Gebhardt, K., Fiedler, H. P., and Jung, G. (2002) Arylomycins A and B, new biaryl-bridged lipopeptide antibiotics produced by *Streptomyces* sp. Tu 6075. II. Structure elucidation. *J. Antibiot. (Tokyo)* 55, 571–577.
- Kulanthaivel, P., Kreuzman, A. J., Strega, M. A., Belvo, M. D., Smitka, T. A., Clemens, M., Swartling, J. R., Minton, K. L., Zheng, F., Angleton, E. L., Mullen, D., Jungheim, L. N., Klimkowski, V. J., Nicas, T. I., Thompson, R. C., and Peng, S. B. (2004) Novel lipoglycopeptides as inhibitors of bacterial signal peptidase I. *J. Biol. Chem.* 279, 36250–36258.
- Paetzel, M., Goodall, J. J., Kania, M., Dalbey, R. E., and Page, M. G. (2004) Crystallographic and biophysical analysis of a bacterial signal peptidase in complex with a lipopeptide-based inhibitor. *J. Biol. Chem.* 279, 30781–30790.
- Li, T., Froeyen, M., and Herdewijn, P. (2008) Computational alanine scanning and free energy decomposition for *E. coli* type I signal peptidase with lipopeptide inhibitor complex. *J. Mol. Graphics Modell.* 26, 813–823.
- Choo, K. H., Tong, J. C., and Ranganathan, S. (2008) Modeling *Escherichia coli* signal peptidase complex with bound substrate: determinants in the mature peptide influencing signal peptide cleavage. *BMC Bioinf.* 9 (Suppl. 1), S15.
- Roberts, T. C., Smith, P. A., Cirz, R. T., and Romesberg, F. E. (2007) Structural and initial biological analysis of synthetic arylomycin A2. *J. Am. Chem. Soc.* 129, 15830–15838.
- Paetzel, M., Chernai, M., Strynadka, N. C., Tschantz, W., Cao, G., Dalbey, R. E., and James, M. N. (1995) Crystallization of a soluble, catalytically active form of *Escherichia coli* leader peptidase. *Proteins* 23, 122–125.
- Hinchliffe, P. S., Wood, J. M., Davis, A. M., Austin, R. P., Beckett, R. P., and Page, M. I. (2003) Structure-reactivity relationships in the inactivation of elastase by beta-sultams. *Org. Biomol. Chem.* 1, 67–80.
- Rosse, G., Kueng, E., Page, M. G., Schauer-Vukasinovic, V., Giller, T., Lahm, H. W., Hunziker, P., and Schlatter, D. (2000) Rapid identification of substrates for novel proteases using a combinatorial peptide library. *J. Comb. Chem.* 2, 461–466.
- Otwinowski, Z., and Minor, W. (1997) Processing of X-ray Diffraction Data Collected in Oscillation Mode. *Methods Enzymol.* 276, 307–326.
- Matthews, B. W. (1968) Solvent content of protein crystals. *J. Mol. Biol.* 33, 491–497.
- Number4, C. C. P. (1994) The CCP4 suite: programs for protein crystallography. *Acta Crystallogr., Sect. D: Biol. Crystallogr.* D50, 760–763.
- Claude, J. B., Suhre, K., Notredame, C., Claverie, J. M., and Abergel, C. (2004) CaspR: a web-server for automated molecular replacement using homology modelling. *Nucleic Acids Res.* 32, 606–609.
- van Aalten, D. M., Bywater, R., Findlay, J. B., Hendlich, M., Hooft, R. W., and Vriend, G. (1996) PRODRG, a program for generating molecular topologies and unique molecular descriptors from coordinates of small molecules. *J. Comput.-Aided Mol. Des.* 10, 255–262.
- McRee, D. E. (1999) XtalView/Xfit - A versatile program for manipulating atomic coordinates and electron density. *J. Struct. Biol.* 125, 156–165.
- Emsley, P., and Cowtan, K. (2004) Coot: Model-Building Tools for Molecular Graphics. *Acta Crystallogr., Sect. D: Biol. Crystallogr.* 60, 2126–2132.
- Brunker, A. T., Adams, P. D., Clore, G. M., Delano, W. L., Gros, P., Grosse-kunstleve, R. W., Jiang, J. S., Kuszewski, J., Nilges, I., Pannun, S., Read, R. J., Rice, L. M., Simonson, T., and Warren, G. L. (1998) Crystallography and NMR System (CNS): A New Software System For Macromolecular Structure Determination. *Acta Crystallogr. D54*, 905–921.
- Painter, J., and Merritt, E. A. (2006) Optimal description of a protein structure in terms of multiple groups undergoing TLS motion. *Acta Crystallogr. D26*, 439–450.
- Laskowski, R. A., MacArthur, M. W., Moss, D. S., and Thornton, J. M. (1993) PROCHECK: a program to check the stereochemical quality of protein structures. *J. Appl. Crystallogr.* 26, 283–291.
- Maiti, R., Van Domselaar, G. H., Zhang, H., and Wishart, D. S. (2004) SuperPose: a simple server for sophisticated structure superposition. *Nucleic Acids Res.* 32, W590–W594.



32. Binkowski, T. A., Naghibzadeh, S., and Liang, J. (2003) CASTp: computed atlas of surface topography of proteins. *Nucleic Acids Res.* **31**, 3352–3355.
33. no.4, C. C. P. (1994) The CCP4 suite: programs for protein crystallography. *Acta Crystallogr., Sect. D: Biol. Crystallogr.* **D50**, 760–763.
34. Merritt, E. A., and Bacon, D. J. (1997) Raster3D: Photorealistic molecular graphics. *Methods Enzymol.* **277**, 505–524.
35. DeLano, W. L. (2002) The PyMOL molecular graphics System, DeLano Scientific, San Carlos, CA.
36. Paetzel, M., Chernai, M., Strynadka, N., Tschantz, W., Cao, G., Dalbey, R. E., and James, M. N. (1995) Crystallization of a soluble, catalytically active form of *Escherichia coli* leader peptidase. *Proteins* **23**, 122–125.
37. Tschantz, W. R., Paetzel, M., Cao, G., Suci, D., Inouye, M., and Dalbey, R. E. (1995) Characterization of a soluble, catalytically active form of *Escherichia coli* leader peptidase: requirement of detergent or phospholipid for optimal activity. *Biochemistry* **34**, 3935–3941.
38. Page, M. I., Hinchliffe, P. S., Wood, J. M., Harding, L. P., and Laws, A. P. (2003) Novel mechanism of inhibiting beta-lactamases by sulfonylation using beta-sultams. *Bioorg. Med. Chem. Lett.* **13**, 4489–4492.
39. Llinas, A., Ahmed, N., Cordaro, M., Laws, A. P., Frere, J. M., Delmarcelle, M., Silvaggi, N. R., Kelly, J. A., and Page, M. I. (2005) Inactivation of bacterial DD-peptidase by beta-sultams. *Biochemistry* **44**, 7738–7746.
40. Paetzel, M., Dalbey, R. E., and Strynadka, N. C. (2002) Crystal structure of a bacterial signal peptidase apoenzyme: implications for signal peptide binding and the Ser-Lys dyad mechanism. *J. Biol. Chem.* **277**, 9512–9519.
41. Tyndall, J. D., Nall, T., and Fairlie, D. P. (2005) Proteases universally recognize beta strands in their active sites. *Chem. Rev.* **105**, 973–999.
42. Kim, Y. T., Muramatsu, T., and Takahashi, K. (1995) Identification of Trp300 as an important residue for *Escherichia coli* leader peptidase activity. *Eur. J. Biochem.* **234**, 358–362.
43. Luo, Y., Pfuetzner, R. A., Mosimann, S., Paetzel, M., Frey, E. A., Cherney, M., Kim, B., Little, J. W., and Strynadka, N. C. J. (2001) Crystal structure of LexA: A conformational switch for regulation of self-cleavage. *Cell* **106**, 1–10.
44. Paetzel, M., Dalbey, R. E., and Strynadka, N. C. (2002) Crystal structure of a bacterial signal peptidase apoenzyme: implications for signal peptide binding and the Ser-Lys dyad mechanism. *J. Biol. Chem.* **277**, 9512–9519.